

# Content-Preserving Image Stitching with the Regular Boundary Constraint

Yun Zhang, Yu-Kun Lai, *Member, IEEE*, and Fang-Lue Zhang, *Member, IEEE*

**Abstract**—This paper proposes a content-preserving stitching with the regular boundary constraint, which aims to rectangling the panorama images with irregular boundary, while avoiding unexpected distortions in the warping-based processes. In our method, the traditional stitching is improved by considering the regular boundary constraint, and the stitching process is configured to be a two-step global optimization which can be efficiently solved. We first conduct stitching by traditional warping-based optimization, and take the warped meshes as initial conditions of the final stitching. Then, we obtain the irregular boundary from the warped meshes by the polygon boolean operations, and construct piecewise rectangular boundary by analyzing and sorting vertices on the irregular boundary. With the piecewise rectangular boundary constraint, we proceed the second step global optimization which incorporates straight line preserving and regular boundary constraints into the image stitching framework. We further conduct iterative optimization to obtain optimal piecewise rectangular boundary, thus can make the panoramic boundary be close to rectangle as much as possible, while reducing unwanted distortions. We further extend our method to panoramic videos and selfie photography, which integrate the temporal coherence and portrait-preserving into the optimization. Experiments show that our method can efficiently produce visual-pleasing results with regular boundaries, unnoticeable distortions.

**Index Terms**—content-preserving, panorama, irregular boundary, piecewise rectangular, warping.

## 1 INTRODUCTION

THE rapid recent advances in digital visual media mean that the public now capture and produce high-quality images and videos, which has promoted the computer graphics applications that utilise visual data captured by ordinary users. Image/video panorama is one of these successful applications. With the integrated panorama module in their smart phones and portable cameras, people can easily take a panoramic photos simply by moving cameras. It is also the most feasible way to get virtual reality content for immersive vision experiences. However, unlike the well calibrated images captured by professional devices with a camera array, the intrinsic and extrinsic parameters of the images captured by consumer-level devices are difficult to estimate. Thus, a robust image stitching method which directly stitches using the visual content is much more important for the applications designed for the ordinary users.

Recently, a lot of progresses have been made in image stitching. However, due to the casual motion of the handheld cameras, after feature alignment, most stitching results by previous methods have irregular boundaries. To display the full panorama in common screens, or generate free-viewpoint photos from one part of the whole scene recorded by the image collection, we can only show them in rectangular windows.

A simple and direct method is cropping, but it will lose important content of stitched panorama, thus may reduce the impression of wide angle photography. In order to produce panorama images with rectangular boundaries, image completion techniques [1], [2] are used to synthesise the missing region in the panorama's bounding box. However, these methods are not stable, and may fail when there need to be semantic meaningful objects. He et al. [3] proposed a warping based method to rectangling panorama images, which can stably produce visual-pleasing panorama images with rectangular boundaries. But their method suffers from the following problems: (1) The stitching and rectangling are two separated processes, so the latter rectangling step may twist the optimized stitching result, making it hard to get an optimal rectangular panorama. (2) When placing grid meshes in stitched irregular panoramas for rectangling, boundary meshes may contain small holes, see Fig. 2(d) and 3(c). (3) The warping-based method will produce large distortion and destroy the feature alignment, when the scene is not completely shot. Thus, when the gap between the rectangular boundary and irregular panorama boundary is large, or there are holes which are difficult for completion and warping methods to fill, there need to be a better approach to create the panorama with regular boundaries while avoiding distortions.

In this paper, we propose a piecewise rectangling scheme which is incorporated into image stitching framework. We aim to regularize the boundary of stitched panorama, and preserve as much as possible content in a rectangular cropping window. Similar to He et al. [3], the process of generating panorama images with rectangular boundaries is termed as “rectangling”. Our method is based on the following observations: (1) Rectangling and stitching are tightly related, and combination of the two processes may

- Yun Zhang is with the Institute of Zhejiang Radio and TV Technology, Communication University of Zhejiang, Hangzhou, China, 310018.  
E-mail: zhangyun@cu.edu.cn
- Yu-Kun Lai is with the School of Computer Science and Informatics, Cardiff University, Wales, UK, CF24 3AA.  
E-mail: Yukun.Lai@cs.cardiff.ac.uk
- Fang-Lue Zhang is with the School of Engineering and Computer Science, Victoria University of Wellington, New Zealand.  
E-mail: fanglue.zhang@ecs.vuw.ac.nz

help to produce better rectangling panorama in a content-aware manner. (2) The aim of panorama rectangling is to preserve as much as possible image content in a rectangular window while avoiding unexpected distortion, thus the irregular boundary should not be simply optimized to be a single rectangle, but piecewise rectangle, see Fig. 2(c).

We first apply image stitching with the global similarity prior [4], and the warped meshes are initial conditions for our rectangling scheme. Then, We extract the irregular boundary by the polygon boolean operations, and construct the piecewise rectangular boundary constraint by analyzing the vertices and intersections on the irregular boundary. Finally, we construct a global optimization which takes into account the feature alignment, shape preserving, global similarity constraints, straight lines and regular boundary. When the target boundary is simply a rectangle, see Fig. 8, the panoramic image is directly obtained by solving the global optimization. For panorama shot by freely moving cameras, the target boundary can not simply represented by a rectangle, see Fig. 1(f), and we proposed the piecewise rectangular boundary constraint, which is incorporated into the stitching framework, and the final results are obtained by iterative warping based optimization. Our method works well in a variety of cases, and can produce visual-pleasing results with no user interactions. Our piecewise rectangling can help users crop panorama with ease, while preserving as much as possible content in the cropping window and avoiding unwanted distortions, thus can enhance the panoramic viewing experiences.

Contributions of this paper are as follows:

- We propose a global optimization to solve the irregular boundary problem in traditional stitching framework by considering the regular boundary constraint, and further apply our method to panoramic selfie and videos.
- We propose a piecewise rectangling scheme to make the panoramic boundary close to a rectangle as much as possible, while avoid unexpected distortions.

## 2 RELATED WORK

In this section, we briefly review the most related works.

**image stitching.** Image stitching aims to create seamless and natural photo-mosaics, and a comprehensive survey of image stitching algorithms is given in [5]. Brown et al. [6] proposed fully automatic panoramic image stitching, and align multiple images by a single homography. Their method is effective under assumption that camera only rotates around its optical center, images are shot from the same viewpoint and the scenes are nearly planar. However, for images shot by hand-held cameras always contain parallax, which limits the application of their method. Given the limitation of single homography, Gao et al. [7] proposed to use two homographies to perform nonlinear alignment, when the scene is modeled by dominant distant and ground planes. However, their method is only effective when there is no local perspective variations. For better performance in image alignment, Zaragoza et al. [8] proposed as-projective-as-possible(APAP) warps based on moving DLT, and can seamlessly align images with different projective models.

Their method can achieve globally perspective, while allowing local non-projective deviations, thus can deal with some challenging cases. Now APAP [8] has been widely applied for its excellent performance in accurate alignment. In this paper, we also apply APAP for image alignment in stitching. Based on the accurate alignment in APAP [8], Lin et al. [9] combined local homography and global similarity transformation to achieve more continuous and smooth stitching, and provided more natural panorama with less visible parallax and perspective distortion. Li et al. [10] proposed dual-feature warping-based model by combining keypoints and line segment features. However, the 2D model proposed in this paper cannot handle large parallax and depth variation, and it is difficult to determine the line correspondences in images with large parallax. For natural warping in stitching, Chang et al. [11] proposed a parametric warp which combines projective and similarity transformation. By combining APAP [8], their method can provide more accurate alignment, less distortion. Chen et al. [4] proposed natural image stitching with global similarity prior to reduce distortion while keep good alignment. To preserve global similarity, they further proposed schemes to select proper scale and rotation for more natural stitching results. To stitch images with large parallax, Zhang et al. [12] proposed local stitching method, which is based on the observation that overlapping regions do not need to be aligned perfectly. Lin et al. [13] proposed a seam-guided local alignment, and optimal local alignment is guided by the seam estimation. In their method, salient curve and line structures are preserved by local and non-local similarity constraint. Very recently, Li et al. [14] proposed robust elastic warping for parallax-tolerant image stitching. To ensure a robust alignment, they proposed a Bayesian model to remove incorrect local matches. He et al. [3] proposed a content-aware warping to produce rectangular images from stitched panorama. Their method is effective to rectangling irregular boundaries caused by projections and casual camera movements. However, their two-step warping strategy separates stitching and rectangling process, which can not ensure an optimal solution, and their method can not process panoramic scenes that are not completely shot. Inspired by [3], We incorporate rectangling into the stitching framework, and construct global optimization to get piecewise rectangular panoramic images. Our piecewise rectangling method can deal with challenging cases, such as panoramic scenes that are not completely shot.

**video stitching.** Compared with image stitching, video stitching is much more difficult, due to the camera motion, dynamic foreground and large parallax. For static camera settings, such as multi-camera surveillance [15], [16], videos from different cameras are aligned only once, and the main challenge is to avoid ghosting and artifacts caused by moving objects. For moving cameras with relative fixed positions, such as camera arrays fixed on the rig [17], cameras can be pre-calibrated for global stitching of videos, and spatio-temporally coherent warping, minimal distortion are the main challenges due to the motion and parallax. Google streetview [18] also applies moving camera arrays for street view capture and panorama generation. To generate high-quality panorama videos, for videos captures by camera arrays fixed on a rig, Zhu et al. [19] proposed

realtime panorama video blending. Meng et al. [20] proposed multi-UAV surveillance system that supports realtime video stitching. Recently, many researchers focus on stitching algorithm for videos shot by multiple hand-held cameras. El-Saban et al. [21] proposed optimal seam selection blending for fast video stitching, however, they do not consider video stabilization. Lin et al. [22] firstly proposed robust framework stitch videos from moving hand-held cameras, which incorporates stabilization and stitching into a unified framework. Guo et al. and Nei et al. [23], [24] further improve the performance of jointly video stabilization and stitching framework. Their main contributions include: estimation of inter motions between cameras and intra motions in a video; common background identification for multiple input videos. In this paper, we extend our content-preserving image stitching to videos that are captured from unstructured camera arrays [17].

### 3 ALGORITHM

Fig. 1 gives the pipeline of our content-preserving stitching. The input to our approach is a number of images with content overlaps, and the goal is to obtain panoramic images with regular boundaries by our content-preserving stitching. In this paper, the term *regular boundary* refers to the piecewise rectangular boundary. We first perform traditional image stitching, and extract the irregular boundary by polygon boolean operations. Then, we further analyze and sort vertices on the irregular boundary, and construct the piecewise rectangular boundary constraints. With the boundary constraint above, we obtain the piecewise rectangling result by iteratively solving global optimizations. We place quad-mesh on each image, and construct energy functions with constraints on the mesh. After optimization, the stitching results are rendered by image warping and blending. The core of our approach is the unified optimization framework that combines image stitching and rectangling, which contains following steps:

**Preprocessing.** In this step, we first calculate the image match graph using the method proposed in [6], and images that are connected in the match graph are aligned to be panoramas. This automatic match process allows stitching with complex image overlaps. For straight line and global feature preserving, we detect lines in all images using fast line segment detector [25].

**Initial image stitching.** The goal of this step is to initialize our content-preserving stitching, and our regular boundary constraints are based on the analysis of warped meshes after stitching. The stitching strategy in this step is also applied in our global optimization which combines stitching and rectangling. We apply APAP [8] for accurate feature alignment. Inspired by [4], we also add a global similarity term for more natural stitching, and globally minimizing the distortion.

**Irregular boundary extraction.** After the initial image stitching, we extract the contour of each warped mesh, and get the irregular boundary by the polygon boolean Union operation. Then, we analyze and sort vertices and intersections on the irregular boundary. Finally, we set the target rectangular boundary constraints for our piecewise rectangular stitching.

**Piecewise rectangular stitching** With the rectangular boundary constraints above, we construct energy optimization which contains image stitching and regular boundary constraint. After minimizing the energy function, we get the stitching result by warping and blending. For panorama scenes that are not completely shot, we iteratively optimize the stitching result by combining boundary segments connected by steps, which aims to make the panoramic boundary as rectangular as possible.

#### 3.1 Initial image stitching

In this step, images are stitched using traditional method, and the irregular boundary of stitching result is the initial conditions for our piecewise rectangular stitching. Actually, when the gap between the irregular boundary and the target rectangular boundary is too large, it will be very difficult or even impossible for rectangling with unnoticeable distortion. Inspired by [4], we stitch images using the global similarity prior to generate more natural panoramas without too much distortions and limit of field of view. Like previous methods, image stitching is performed by the mesh-based image warping. Let  $V_i$  and  $E_i$  be the vertices and edges in image  $I_i$ , we aim to get deformed vertices  $V$  by minimizing the energy function  $\Phi(V)$ , which contains following terms: feature alignment, local shape and global similarity preserving.

**Feature Alignment.** This term aims to align matched images by preserving the feature correspondences between them. Given the good performance in piecewise alignment, we apply APAP [8] for feature alignment, and the feature alignment constraint is defined as follows.

$$\phi_a(\mathbf{V}) = \sum_{i=1}^N \sum_{(i,j) \in G} \sum_{p_m^{ij} \in M_{ij}} \|\mathbf{V}_{pq}^{ij} \cdot \Omega_{pq}^{ij} - \tilde{\mathbf{V}}_{pq}^{ij} \cdot \tilde{\Omega}_{pq}^{ij}\|^2, \quad (1)$$

where  $G$  refers to the image match graph which determines the matched image pair.  $p_m^{ij}$  represents a pair of matched feature points by matching image  $i$  and  $j$ , and  $M_{ij}$  is the image matching set. Since the constraints are imposed on vertices of the mesh, we employ the bilinear coordinates represent matched feature points as the interpolation of four vertices of a quad grid  $p_m^{ij} = \mathbf{V}_{pq}^{ij} \cdot \Omega_{pq}^{ij}$ , where  $\mathbf{V}_{pq}^{ij} = [V_{p,q}^{ij}, V_{p+1,q}^{ij}, V_{p+1,q+1}^{ij}, V_{p,q+1}^{ij}]$  and  $\Omega_{pq}^{ij} = [\omega_{p,q}^{ij}, \omega_{p+1,q}^{ij}, \omega_{p+1,q+1}^{ij}, \omega_{p,q+1}^{ij}]$ .

**local Shape preserving.** This term aims to ensure that each quad grid in the mesh can undergo a similar transform and do not distort too much. we use the shape preserving term defined in [26], which splits each grid into two triangles and applies the method in as-rigid-as-possible warping [27].

$$\phi_s(\mathbf{V}) = \sum_{i=1}^N \sum_j \|V_j^i - V_1^i - \xi \mathbf{R}(V_0^i - V_1^i)\|^2, \quad (2)$$

where  $\mathbf{R} = \begin{bmatrix} \cos\theta & \sin\theta \\ -\sin\theta & \cos\theta \end{bmatrix}$ ,

and  $\xi = \|V_j^i - V_1^i\| / \|V_0^i - V_1^i\|$ .

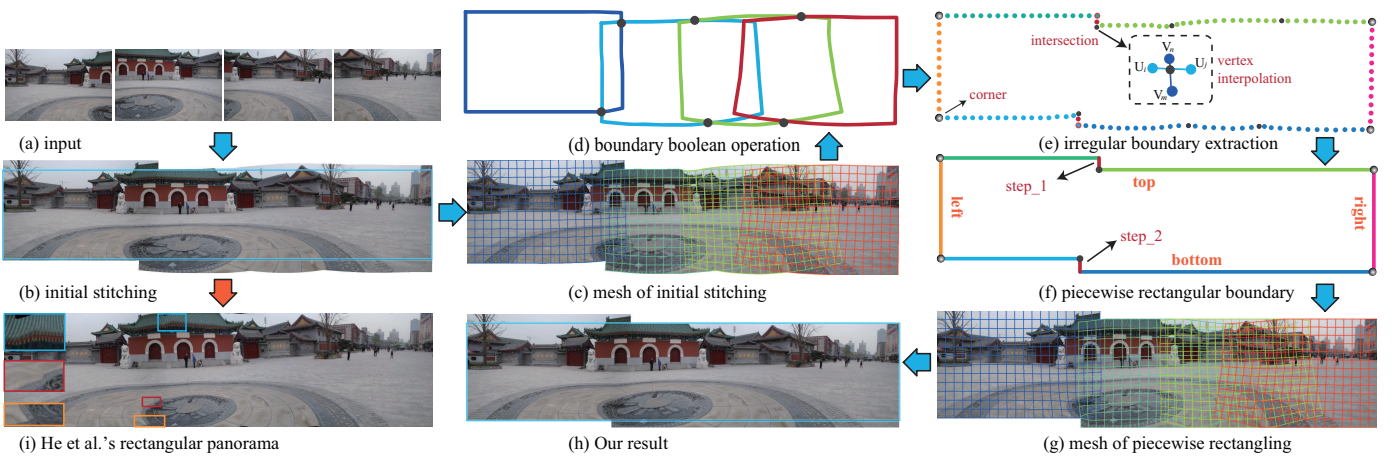


Fig. 1. Pipeline of our stitching with regular boundary. (a) Input images. (b) initial stitching with irregular boundaries. (c) mesh of initial stitching. (d) outer boundary extracted by polygon boolean extraction. (e) irregular boundary extraction. (f) target regular boundary. (g) mesh of piecewise rectangling. (h) our result. (i) He et al.'s rectangular panorama.

In Equ. 2,  $\theta$  refers to the angle formed by moving segments from  $V_1 V_0$  to  $V_1 V$ . When the direction is anticlockwise  $\theta = 90^\circ$ , and  $\theta = -90^\circ$  for the clockwise direction. In our implementation,  $V_0^i$  refers to the top-left vertex of all quads in the image mesh,  $V_0^i$  and  $V_1^i$  are the neighboring vertices of  $V_0^i$  in a triangle.

**Global similarity.** We use the global similarity term proposed in [4], which is important to preserve the naturalness of the panoramic images, and can reduce the gap between the irregular boundary and the target rectangle. We first set a reference image  $I_0$  and its desired rotation  $r_0$ , then for each image, the desired scale  $s_i$  and rotation  $r_i$  with respect to  $I_0$  are calculated, see details in [4]. The global similarity term is defined as

$$\phi_g(\mathbf{V}) = \sum_{i=1}^N \sum_{e_j^i \in \mathbf{E}_i} \alpha(e_j^i) [||c(e_j^i) - s_i \cos \theta_i||^2 + ||s(e_j^i) - s_i \sin \theta_i||^2], \quad (3)$$

In Equ. 3,  $c(e_j^i)$  and  $s(e_j^i)$  refer to the coefficients of grid edges for similarity transform in  $x$  and  $y$  directions, see details in [28].  $\alpha(e_j^i)$  is the weight to assign more importance to the edge in the overlapping region, while less in other area, in order to keep accurate alignment and preserve the naturalness, and it is defined as

$$\alpha(e_j^i) = \frac{\sum_{q_m \in Q(e_j^i)} \text{Min}(d_{cen}(q_m, \Psi_i))}{\sqrt{W_i^2 + H_i^2} \cdot |Q(e_j^i)|}, \quad (4)$$

where  $Q(e_j^i)$  refers to the quads that contain edge  $e_j^i$ ;  $\Psi_i$  is the overlapping region in image  $I_i$ ;  $\text{Min}(d_{cen}(q_m, \Psi_i))$  calculates the minimum distance between the center of quad  $q_m$  and the quads in  $\Psi_i$ ;  $W$  and  $H$  are the number of rows and columns of the mesh in image  $I_i$ .

With the energy terms defined above, we define the optimization for image stitching as

$$\Phi_{stitch}(V) = \arg \min_V (\gamma_a \phi_a(V) + \gamma_s \phi_s(V) + \gamma_g \phi_g(V)). \quad (5)$$

In Equ. 5, there are three weights  $\gamma_a$ ,  $\gamma_s$ ,  $\gamma_g$ , which controls the importance of the three terms. In our experiments,

we set  $\gamma_a = 1.5$ ,  $\gamma_s = 10$ ,  $\gamma_g = 0.75$  for most of the cases. The stitching energy  $\Phi(V)$  are quadratic and can be efficiently minimized by solving a sparse linear system.

### 3.2 Irregular boundary extraction

Different from [3], which uses only one mesh for warping based rectangling, our rectangling scheme starts from the warped meshes of each stitched image. The irregular boundary consists of vertices from different image meshes, and intersections of overlapped meshes, see Fig. 1(d). Inspired by the boolean operations on polygons [29], we propose a simple and effective algorithm for irregular boundary extraction. See Alg. 1, the input is the mesh vertices  $V_i$  of each warped image  $I_i$ , and the goal is to get irregular boundary vertices and their labels. We first get minimum outer rectangle  $R$  of all warped meshes, and obtain 4 corners of irregular boundaries according to the minimum distance between corners of each mesh  $V_i$  and  $R$ . Then, we construct polygons  $\vartheta$  using the contours of each mesh, and the irregular boundary can be efficiently calculated by the polygon boolean union operation of all boundary polygons. With corners  $\Delta$  and boundary polygon  $P$ , the boundary vertices of 4 directions can be easily obtained by sequentially collecting vertices between neighboring corners of  $P$ . As shown in Fig. 1, the initial image stitching result has irregular boundary which is the combination of 4 image meshes. Fig. 1(b) shows contours of all meshes, and each contour has a different color. The black circles are intersections of these contours. As shown in Fig. 1(c), after the polygon boolean union operations, the irregular boundaries  $V^R$  are correctly extracted and classified into 4 directions. For the intersection points, which cannot be treated as vertices. We first detect the corresponding intersected vertices  $\kappa$ , and calculate the interpolation weight of the vertices  $\eta$ , then the intersection points can be easily constrained by the neighboring vertices.

### 3.3 Piecewise rectangular boundary constraint

For panoramic scenes with missing content, He et al.'s [3] warping-based rectangling cannot work well, as it may introduce unexpected distortions after too much warping,

**Algorithm 1:** Irregular boundary extraction

---

**Input:** Mesh vertices  $V_i$  of each warped image  $I_i$ ,  
 $i = 1, 2, \dots, N$

**Output:** boundary vertices  $V^{\mathcal{R}}$  and their labels  $\zeta$

Get minimum outer rectangle  $R$  of all meshes;  
Set  $D_{min} = Dist(Corners(R), Corners(V_i))$ ;  
construct polygon  $\vartheta_1$  using contour vertices of mesh  
 $V_i$ ;  
Set  $P = \vartheta_1$ ;  
Set boundary corners  $\Delta = Corners(V_1)$ ;

**for** ( $i = 2; j \leq N; j++$ ) **do**

- Construct polygon  $\vartheta_i$  using contour vertices of  $I_i$ ;
- Polygon boolean Union:  $P = P \cup \vartheta_i$ ;
- if** ( $dist(Corners(R), Corners(V_i)) < D_{min}$ ) **then**

  - $\Delta = Corners(V_i)$ ;
  - $D_{min} = Dist(Corners(R), Corners(V_i))$ ;

- end**

**end**

**for** ( $j = 1; j \leq size(P); j++$ ) **do**

- if** ( $P[j] \in vertices$ ) **then**

  - $\zeta[P[j]] = 1$ ;

- end**
- else if** ( $P[j] \in intersections$ ) **then**

  - $\zeta[P[j]] = 0$ ;
  - $\kappa[P[j]] = [V_m, V_n, V_p, V_q]$ ;
  - $\eta[P[j]] = [C_m, C_n, C_p, C_q]^T$ ;

- end**

**end**

Get boundary vertices between neighboring corners of  $P$ ;

**for** ( $k = 1; k \leq 4; k++$ ) **do**

- $V^{\mathcal{R}}[k] = P(\Delta(k), \Delta((k+1)\%4))$ ;

**end**

---

see Fig. 1(i). Actually, panorama images with irregular boundary cannot simply be warped to be a rectangle, and the rectangling process should be content-aware. In this paper, we propose the piecewise rectangling scheme which makes the target boundary as rectangular as possible, while avoiding the unwanted distortions. See Fig. 1(h), with the piecewise rectangular boundary, the panoramic image can be cropped easily, while preserving more content in a cropping window.

Alg. 2 gives details of piecewise regular boundary analysis. The input is mesh vertices of irregular boundaries  $V^{\mathcal{R}(k)}$ , and output is the segmented boundary  $S$ . The irregular boundaries are comprised of boundary vertices from different image meshes, which are connected by their intersections. We first segment the  $V^{\mathcal{R}(k)}$  by intersections and corner vertices (with red boundary in Fig. 1(e)) of each mesh. Then we combine neighboring segments with the same direction, and incorporate segments with less than 3 vertices into previous segment. After analyzing and sorting the irregular boundaries, we calculate the target boundary value of each segment by averaging their coordinates in corresponding direction. See Fig. 1(f), the top and bottom boundary contain 3 segments, and the steps are designed to reduce distortions in global warping.

**Algorithm 2:** Piecewise regular boundary analysis

---

**Input:** Vertices  $V^{\mathcal{R}}$  on the irregular boundary

**Output:** Segmented boundary  $S$ , includes vertices, directions( $1 - y, 0 - x$ ), and their target boundary values

Sequentially push intersections and corner points into  $F$  in 4 directions; Segment irregular boundary  $V^{\mathcal{R}}$  by  $F$ ;

Set  $prevDir = i$ ;

**for** ( $i = 1; i <= 4; i++$ ) **do**

- for** ( $j = 1; j \leq size(F); j++$ ) **do**

  - $S_j^i = V^{\mathcal{R}}(F[j], F[j+1])$ ;
  - $S_j^i.dir =$ direction of  $(F[j], F[j+1])$  in meshes;

- end**
- for** ( $j = 1; j <= size(S^i); j++$ ) **do**

  - if** ( $S^i[j].dir == prevDir \& \& j > 1$ ) **then**

    - $S^i[j] \rightarrow S^i[j-1]$ ;

  - end**
  - else**

    - if** ( $dist(S^i[j], S^i[j-1]) < \varepsilon$ ) **then**

      - $S^i[j] \rightarrow S^i[j-1]$ ;

    - end**
    - else**

      - $prevDir = S^i[j].dir$ ;

    - end**

  - end**
  - if** ( $S^i[j].dir \% 2$ ) **then**

    - $S^i[j].val = Avg(V^{\mathcal{R}}(S^i[j]).y)$ ;

  - end**
  - else**

    - $S^i[j].val = Avg(V^{\mathcal{R}}(S^i[j]).x)$ ;

  - end**

**end**

---

### 3.4 Piecewise rectangular stitching

We design a global optimization which incorporate rectangling into image stitching framework. Our energy function contains constraints for image stitching, such as feature alignment, local shape and global similarity preserving, and constraints for rectangling, such as regular boundary, straight line preserving. The energy terms for stitching have been defined in Section 3.1, and we further define energy terms for irregular boundary rectangling as follows.

**Regular boundary preserving.** With the piecewise rectangular boundary constraint defined in Section 3.3, we define the regular boundary preserving energy as

$$\phi_r(\mathbf{V}) = \sum_{i=1}^4 \sum_{j=1}^{size(S^i)} \sum_{V_k \in S^i[j]} \|\Lambda(S^i[j])^i [\zeta[V_k]V_k + (1 - \zeta[V_k]) (\kappa[V_k] \cdot \eta[V_k])] - S^i[j].val\|^2, \quad (6)$$

where  $S$  represents all boundary segments, and  $S^i[j].val$  refers to the values of each target boundary segment;  $\zeta[V_k]$  determines the type of vertices: 1 - vertices, 0 - intersections;  $\Lambda(S^i[j])$  is the  $2 \times 1$  matrix, and  $\Lambda(S^i[j]) = [0 \ 1]$  or  $[1 \ 0]$ , when  $S^i[j]$  is horizontal or vertical. For intersection

points, we find their neighboring vertices  $\kappa$  that generate the intersections, and their corresponding interpolation weights  $\eta$ , then constraints are imposed on these vertices.

**Straight line preserving.** To avoid unexpected distortion after warping, we also need to preserve straight lines in panoramas. We use the line preserving term from [22], and the line segments detectors are proposed in [25]. Given the line segments, our energy term is defined as

$$\phi_l(V) = \sum_{i=1}^N \sum_{l \in L_i} \sum_{j=1}^{M-1} \left\| (1-\mu)V_{l,0}^i \omega_{l,0}^i + \mu V_{l,M}^i \omega_{l,M}^i - V_{l,j}^i \omega_{l,j}^i \right\|^2, \quad (7)$$

where  $M$  is the number of sub-segments for each line segment, and each sample point on the line segment is represented by the bilinear interpolation of the 4 grid vertices. The two end points are represented as  $V_{l,0}^i \omega_{l,0}^i$ ,  $V_{l,M}^i \omega_{l,M}^i$ , and the sample point between the end points is  $V_{l,j}^i \omega_{l,j}^i$ . The linear combination of them can easily preserve the straight lines, and the weight  $\mu = j/M$ .

With the piecewise regular boundary and straight line preserving constraints, the energy function for content-preserving image stitching with regular boundary can be defined as

$$\Phi(V) = \Phi_{stitch}(V) + \gamma_r \phi_r(V) + \gamma_l \phi_l(V), \quad (8)$$

where  $\Phi_{stitch}$  is the stitching energy function defined in Section 3.1,  $\gamma_r$  and  $\gamma_l$  are weights to control the importance of energy terms. We set  $\gamma_r = 10^3$  to ensure the regularity of boundaries. In our experiment, we find that the line preserving is more important than the local shape preserving, thus  $\gamma_l$  is set to be 20 to avoid too much distortions in straight lines.

### 3.5 Optimization

We first solve optimization for the initial image stitching, which is defined in Equ. 5. However, Equ. 5 only constrains shape and scale of each mesh, which is not enough for stitching. Thus, we add another term  $\phi_p(V) = W \cdot \|V_0^0\|^2$  to fix the position of stitched panorama, where  $V_0^0$  refers to the first vertex(left-top corner) of the first image, and  $M$  is a very large weight ( $M = 10^4$ ) to make  $\phi_p$  a hard constraint. Noting that, each energy term is quadratic and variables are mesh vertices of each image, the energy function can be efficiently optimized by solving a linear system. Since this stitching step is only used to get the target rectangle and irregular boundary, we do not need to render the stitching result by warping and blending.

After the irregular boundary extraction, we solve the optimization defined in Equ. 8 which incorporates the regular boundary and straight line constraint into the stitching framework. Compared with initial image stitching, we add another two energy terms, which are also quadratic, thus the optimization can also be efficiently minimized.

With the optimized vertices of each mesh, we further warp each image by texture mapping and remove the visible seam by multibanded blending [19]. For efficiency, we can also simply apply the linear blending, which can work well in most cases. Fig. 1(i) is stitching results constrained by piecewise rectangular boundary. Compared with previous

rectangling [3], it makes a better balance between distortion and rectangling.

In this paper, we aim to rectangling the panorama with irregular boundary as much as possible, which means the final shape of the panorama should be as close as possible to a rectangle. Thus, we try to further reduce steps on the piecewise rectangular boundary. We propose an iterative solution which is described in Alg. 3. The first iteration has been accomplished by the optimization above, see Fig. 2(f), and we calculate the energy values  $E_0$  using the optimized vertices. Then we iteratively find the optimal solution, that can preserve regular boundary as much as possible while avoiding unwanted distortion. In the following iteration, for each step, we first analyze feature points and lines detection results near the boundary segments connected by the step, and when there are some detected features and lines, the step cannot be removed. See Fig. 1(h), we preserve the two steps because of the features and lines distributed in the roof and ground. When feature and lines are not salient, such as grass and sky, we further analyze it as follows: for each step, we connect the segments neighboring to it, and reconstruct all segments  $S$ , then perform image stitching again, finally we choose to remove the step with the minimum energy value  $E$ . In each iteration, the threshold  $\sigma = |E_t - E_0|/20$ , according to many experiments. When the energy value  $E_t - E_0 > \sigma$ , it means that energy varies too much compared with last iteration, thus it is not acceptable. Then the iteration stops, and we finally get the optimal solution for the piecewise rectangling. Actually, the panorama rectangling proposed by He et al. [3] can be classified as a special case of our piecewise rectangling, when there is no steps in the target boundaries. Fig. 2 (e) is the rectangling result by our method when all steps are removed, and there exists too much distortions in the bottom-right side. Compared with He et al.'s [3] result in Fig. 2 (d) which contains holes and distortions, our rectangling result is better. Fig. 2(f-i) are results of piecewise rectangling in each iteration, and the top-right corner shows the shape of target regular boundary. Results show that each iteration can make the boundary of panorama be closer to a rectangle, and finally we get panorama with optimal piecewise rectangular boundary and unnoticeable distortions.

## 4 RESULTS AND APPLICATIONS

In this section, we show a variety of panoramic images by image stitching with regular boundary constraint, and applications that benefit from our approach. Then we further give performance and limitation of our method. In this paper, we use the dataset provided by Chen et al. [4] for image stitching, and the data for video stitching is from Perazzi et al.'s paper [17]. For better exposition, we only provide input for examples provided by ourselves.

### 4.1 Results

Fig. 3 is the comparison of our method with He et al.'s method [3]. For fair comparison, the input of He et al.'s [3] method is our initial stitching which has irregular boundary. The left initial stitching is the first step of our method. As shown in the comparison, the main difference between

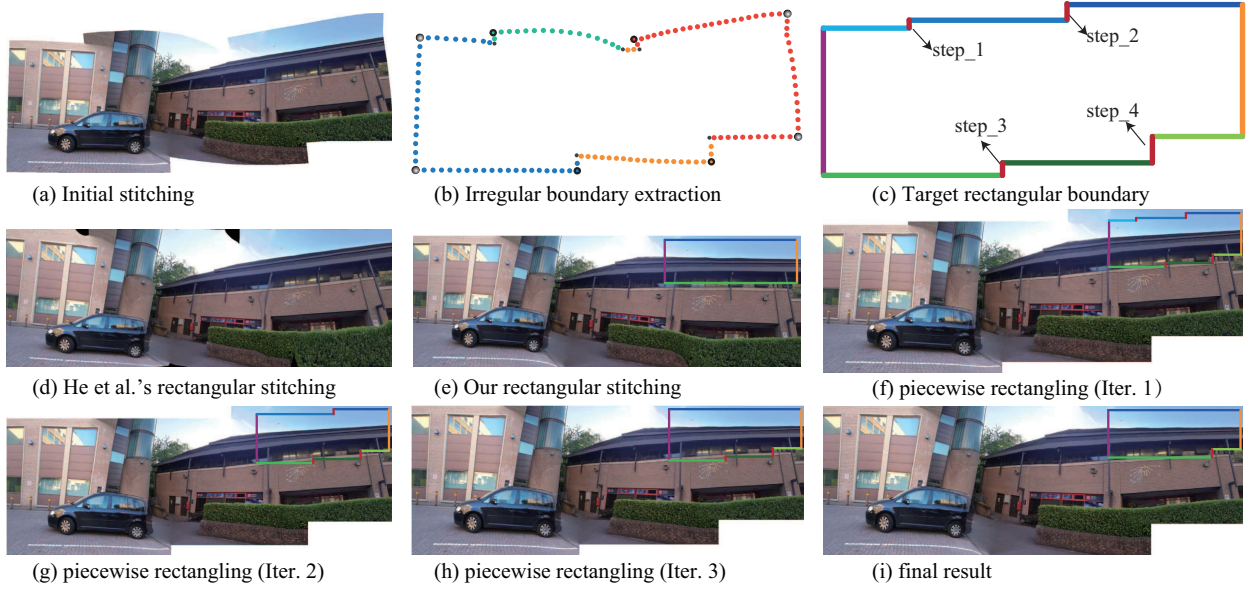


Fig. 2. Piecewise rectangling in image stitching. (a) Initial stitching result with irregular boundary. (b) Irregular boundary extraction. (c) Target boundaries estimation. (d) He et al.'s [3] rectangular stitching result. (e) Our rectangular stitching result. (f i) stitching results by iterative piecewise rectangling, and (i) is our final stitching result.

### Algorithm 3: Iterative piecewise rectangling stitching

```

Input: Source images,  $S$  refers to segments of the
      piecewise rectangular boundary, and  $P$ 
      represents steps that connect all segments
Output: Stitching result with optimized regular
      boundary
Init: Perform stitching with  $S$  as boundary constraints;
 $E_0 = \Phi(V)$ , where  $V$  is the optimized vertices;
while ( $1$ ) do
     $Idx = 0, E_t = 10^6$ ;
    for ( $k = 0; k < \text{size}(P); k++$ ) do
        segments connected by  $P[k]$ ;
        reconstruct  $S$ ;
        Stitching with  $S$  as boundary constraints;
         $E = \Phi(V)$ ;
        if ( $E < E_t$ ) then
             $| Idx = k;$ 
             $| E_t = \Phi(V);$ 
        end
    end
    if ( $(E_t - E_0) < \sigma$ ) then
         $| \text{remove } P[Idx];$ 
         $| E_0 = E_t;$ 
    end
    else
         $| \text{break};$ 
    end
    if  $\text{size}(P) == 0$  then
         $| \text{break};$ 
    end
end

```

the two method is the number of mesh used in the global warping. Actually, it is hard to place mesh on images with irregular boundary, and the boundary of the mesh always contain some holes(see bottom side of Fig. 3(a) and (b)), which will finally degrade the quality of the final rectangular panorama, see the zoom-in view in Fig. 3(c). In addition, He et al's method treat stitching and rectangling as two individual processes, thus cannot well preserve the local and global structure of the panorama. In our method, the meshes are placed on the each rectangular images, and the warping are guided by the global optimization which combines stitching and rectangling constraints, thus can produce stitching with regular boundaries while reducing the local and global distortion, see Fig. 3(f).

Fig 4 gives comparison with state-of-the-art methods in terms of line preserving. In Chen et al.'s method [4], their line segment detection is used for global feature preserving, like scale and rotation, but they cannot preserve straight lines, as shown in (a). He et al.'s method is limited to the input, and when the input panorama fails to preserve straight lines, their method also fails, see the arrows in Fig 4(b). Fig 4(c) and (d) are the initial piecewise rectangular stitching results with and without line preserving, and results show that our method can well preserve straight line in our optimization framework. Fig 4(e) is the final result after several iterations, which not only preserves lines, but avoid unexpected distortions.

Fig. 5 gives results and comparison of stitching with missing contents in the scene. We provide two groups of experiments to show the effectiveness of our method in challenging cases. Fig. 5(a) is the initial stitching results, which is also the input of He et al.'s [3] method. Fig. 5(b) and (c) show the meshes after initial stitching and the extracted irregular boundaries. Fig. 5(d) and (e) are the rectangular stitching results by He et al.'s and our method. Although both (d) and (e) have severe distortions, our result is more

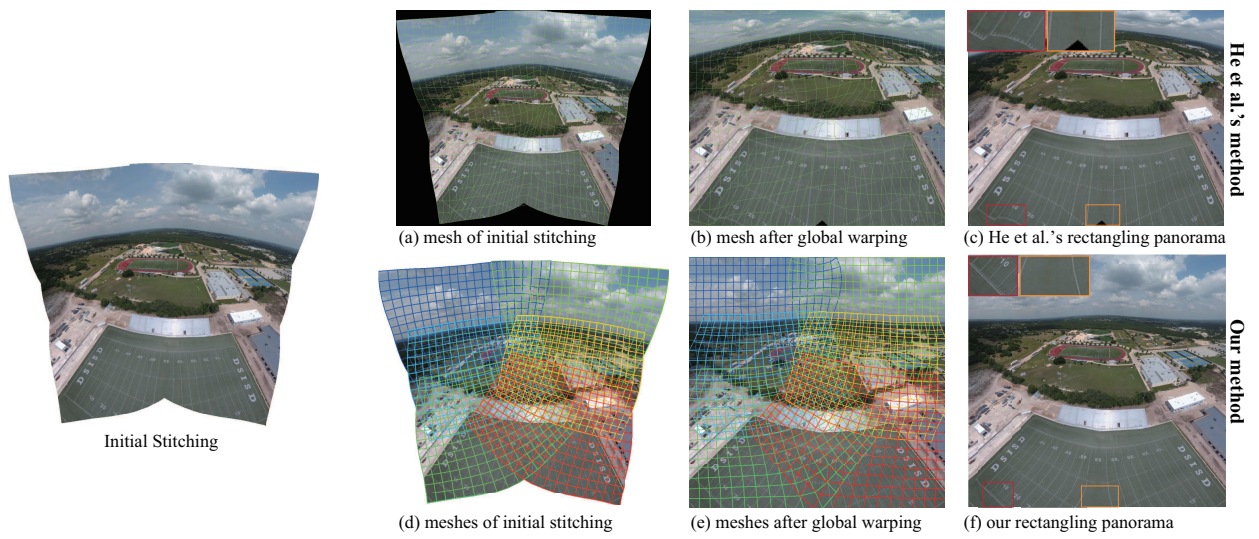


Fig. 3. Comparison with He et al.’s method [3]. The initial stitching is the first step of our method, which is also the input of He et al.’s method [3]. For He et al.’s method: (a) mesh of on the input image; (b) mesh after global warping; (c) final rectangular panorama. For our method: (d) meshes of our initial stitching; (e) meshes after the global warping; (f) our rectangular panorama.

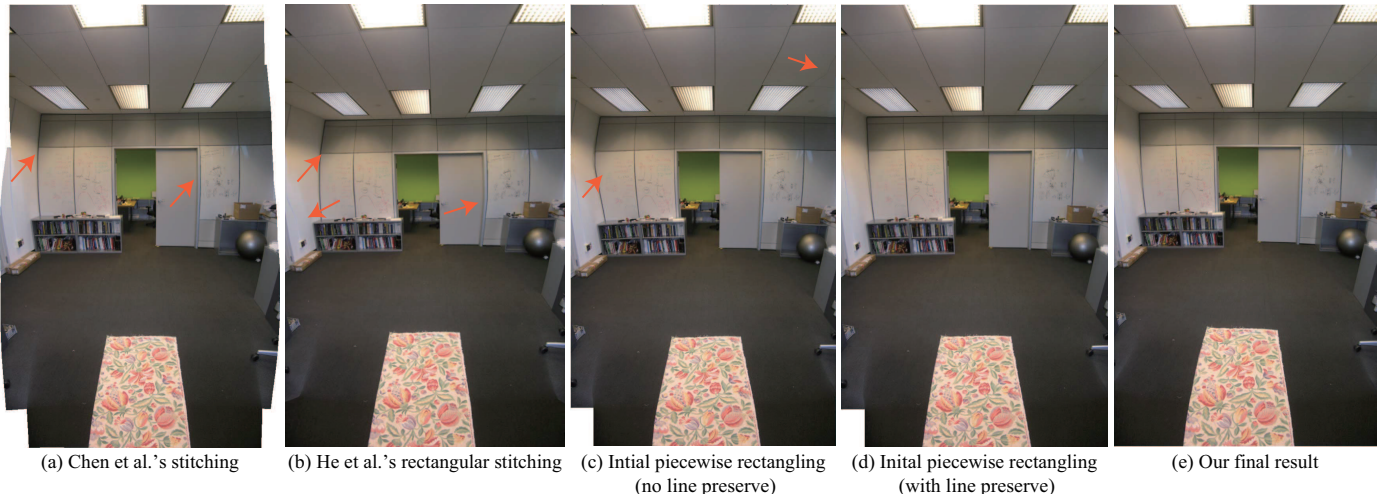


Fig. 4. Comparison with state-of-the-art methods. (a) Chen’s [4] stitching with global prior. (b) He et al.’s [3] rectangling stitching. (c) and (d) are Our piecewise rectangling results in the 1<sub>st</sub> iteration with and without line preserving. (e) our final stitching results after several iterations.

reasonable and visual pleasing. In addition, the result by He et al.’s method has holes, due to the drawbacks of their mesh placement. Fig. 5(f) is our piecewise rectangling result, which is the optimal panorama with less distortion, and can preserve the content of panorama in the rectangular window as much as possible.

Fig. 6 shows comparison with image completion. Fig. 6(a) is the initial stitching result. By completing holes in Fig. 6(a) using Huang et al.’s [30] method, we get rectangular panorama as shown in Fig. 6(c). Zoom-in view in Fig. 6(c) shows that the completion method is limited to synthesize semantic contents. Fig. 6(b) is the piecewise rectangling method, and our method tries the best to preserve regular boundaries while preventing unwanted distortions. Based on our piecewise rectangling result, we apply Huang et al.’s [30] method to complete the rectangular hole on the left, and result in Fig. 6(d) shows that the combination of our method and completion is more successful than the

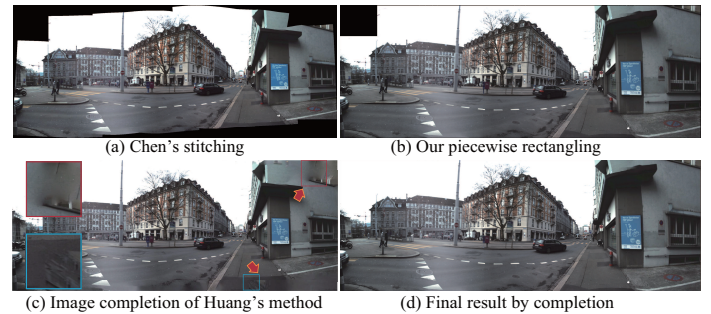


Fig. 6. Comparison with image completion. (a) is the result of initial stitching. (b) shows our piecewise rectangling panorama.(c) is the result by Huang et al.’s [30] image completion. (d) our final result which is generated by completing holes in (b).

completion alone.

Fig. 7 gives results of challenging cases, and each case

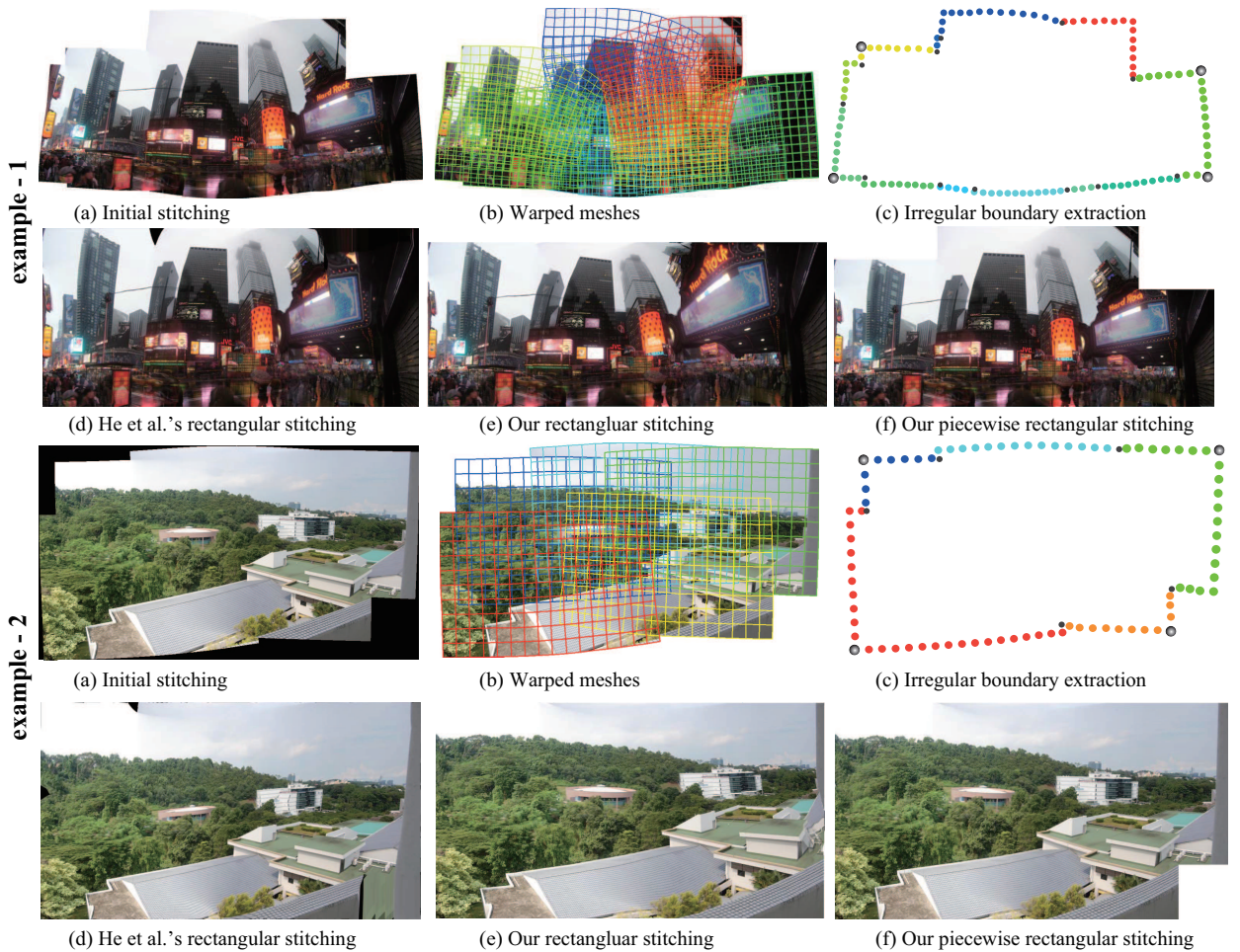


Fig. 5. Results and comparison of stitching with missing contents. There are two sets of results, and each set is as follows: (a) Initial stitching result with irregular boundaries. (b) Warped meshes of initial stitching. (c) Irregular boundary extraction. (d) and (e) are rectangling stitching by He's [3] and our method respectively. (f) our piecewise rectangular stitching result.

is very different from common examples. The first row is results of initial stitching result with irregular boundaries, and the second row shows our piecewise rectangling panorama. With the piecewise rectangular boundaries, the panoramic images can be easily cropped and completed, thus can improve the visual effects and viewing experience of panorama.

## 4.2 Applications

### 4.2.1 Selfie expansion

Recent years, with the fast development of intelligent devices such as smart phones, pad etc., selfies have become more and more popular. In general, selfie images are mostly shot by mobile phones by holding them or fixing them to selfie sticks. Since the camera is very close to people, the selfie photos are always limited by the field-of-view, thus may reduce the fun of selfies. To produce selfies with large field-of-view, we apply our image stitching to producing selfie panorama. Actually, the front-facing camera which is used for selfie shooting, can not shoot a panorama view. We first take photos of the panorama view using the back camera, then shot our portrait using the front-facing camera on the background of the panorama. See Fig. 9, (a) is the input, which contains photos for the panorama background,

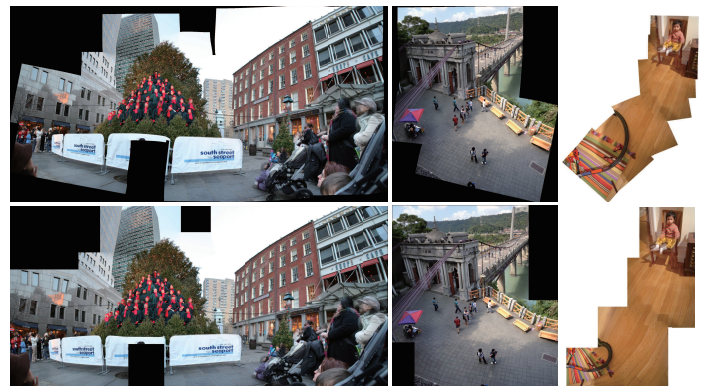


Fig. 7. Results of challenging cases. The 1<sup>st</sup> row shows Initial stitching results with irregular boundaries, and the 2<sup>nd</sup> row shows results of our piecewise rectangling stitching.

and the portrait photo. (b) is the result by Chen et al.'s stitching [4], which contains irregular boundaries. (c) is result by our method, and the red rectangle shows distortion on the human face. To fix this problem, we first detect the

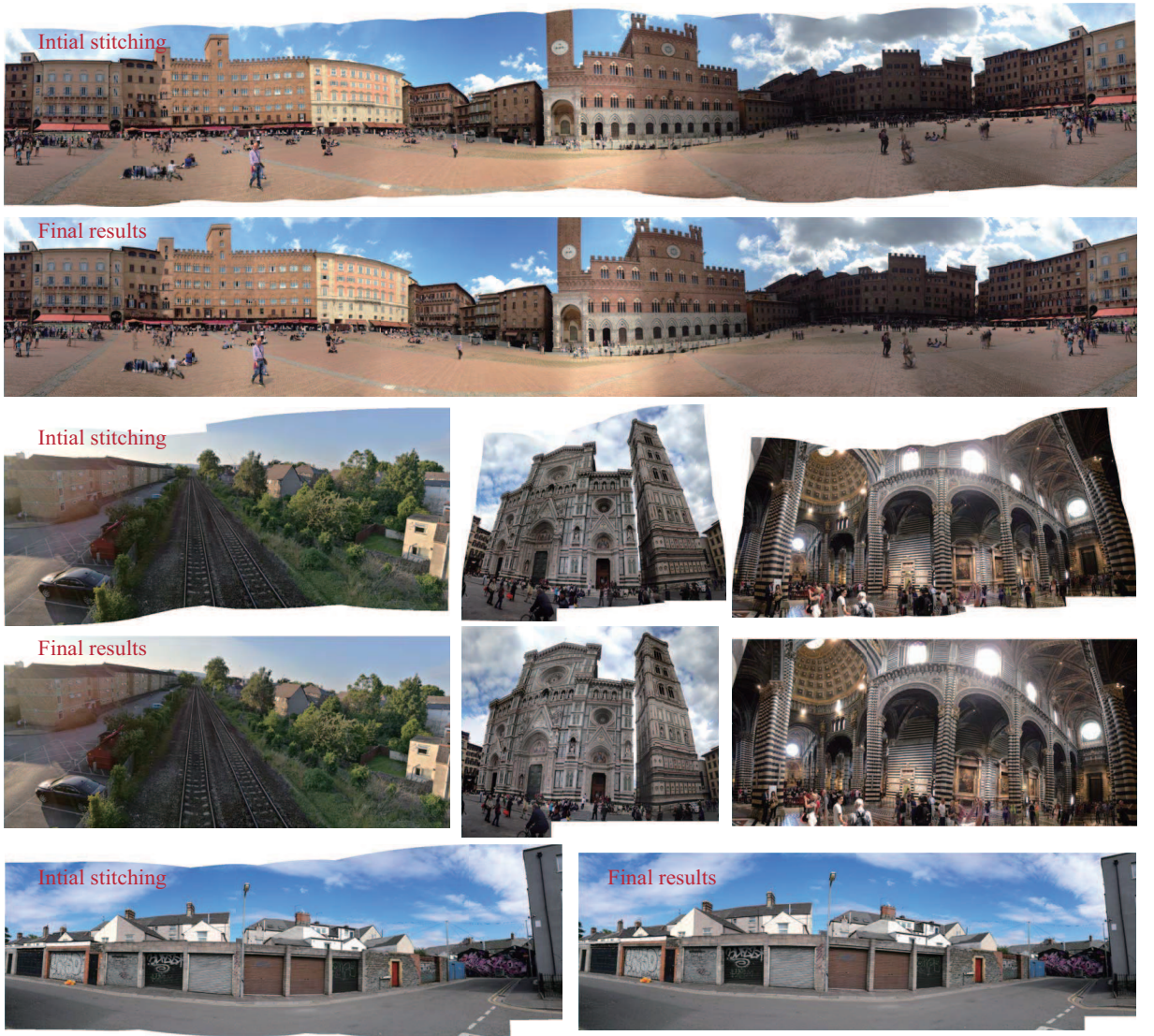


Fig. 8. More results of our method. The initial stitching is traditional method without the regular boundary constraint, and final results are obtained by our rectangular stitching.

face the portrait photo, and modify Equ. 2 as

$$\phi_s(\mathbf{V}) = \sum_{i=1}^N \sum_j \alpha_j^i \|V_j^i - V_1^i - \xi \mathbf{R}(V_0^i - V_1^i)\|^2, \quad (9)$$

where  $\alpha_j^i$  refers to the saliency value of vertex  $V_j^i$ , we give a big value ( $\alpha_j^i=20$ ) for vertices in the face region, and 1 for others. By preserving the shape of mesh in the face region, the stitching result is much more visual pleasing, as shown in (d).

#### 4.2.2 Rectangling Video Panorama

We further apply our method to videos stitching. Actually, it is difficult to stitch the videos from independent hand-held cameras, and rectangling them is even more challenging. Because the regular boundary in each frame is different and the temporal coherence is difficult to maintain due to the shaking in each video. Inspired by Perazzi et al.'s [17] work, we aim to rectangling panorama videos from unstructured camera arrays, which are fixed on a rag. For fixed camera

configurations, the warping parameters for stitching in each frame are nearly invariant. For temporal coherence, we propose a simple and effective scheme as follows. We first divide videos into several blocks (1 block=30 frames), and neighboring block has 10 frames overlap. For each block, we compute the stitching result for the first frame, and the warping parameters are used for other frames. For the overlapping part, the warping parameters are linear combination of neighboring blocks. Fig. 10 shows two sets of results, and each set shows video panoramas of 4 frames by Perazzi et al.'s [17] and our method. Comparison shows that our method is effective to rectangling video panorama shot by fixed camera arrays, and can provide better view experience.

#### 4.3 Performance

We report performance of our method on a Intel Core i7 8550U 1.99GHz laptop with 16G RAM for examples in this paper. Take Fig.1 for example, the input contains 5 images, and size of each image is  $800 \times 600$ , the initial

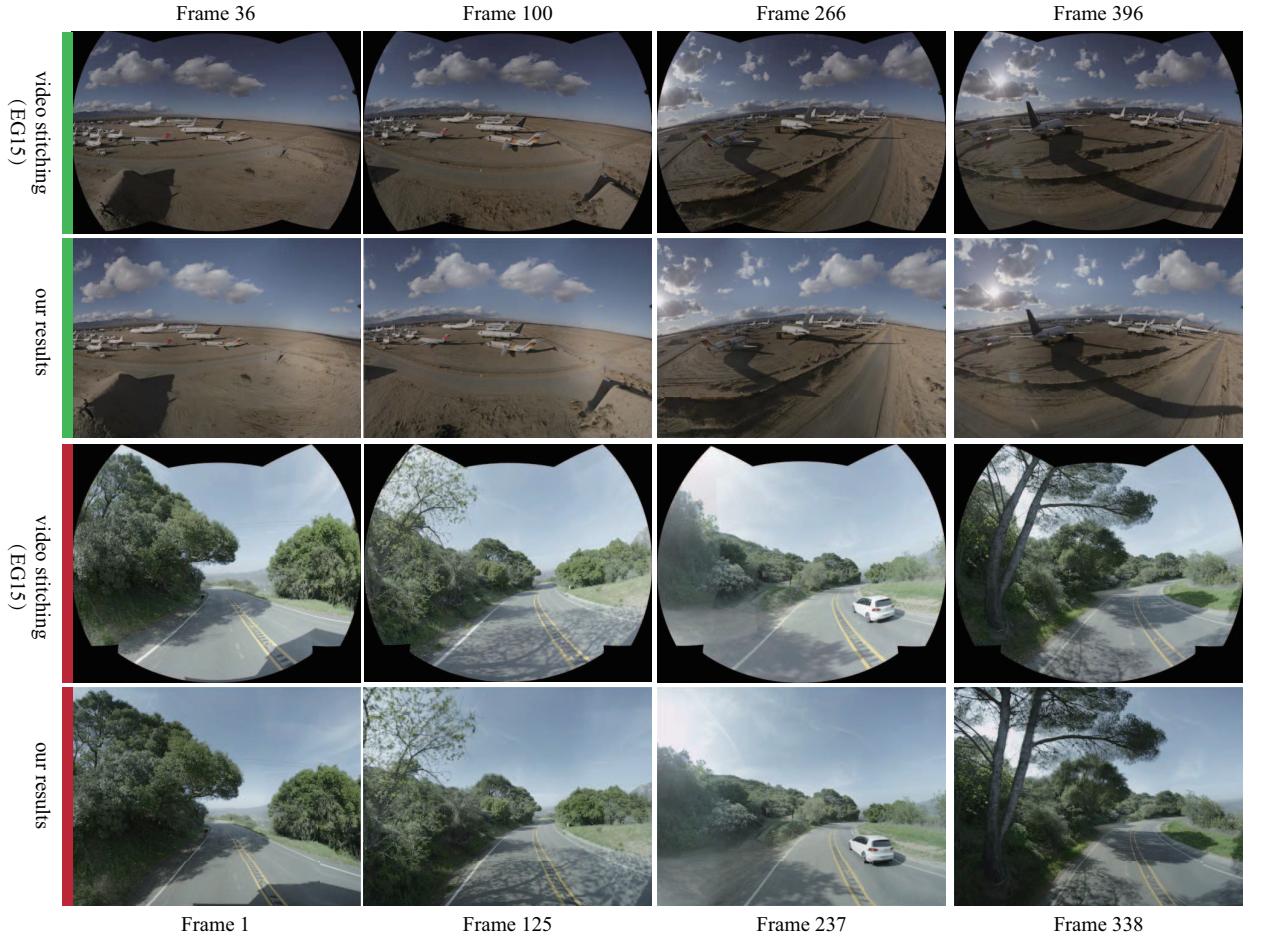


Fig. 10. Application of rectangling video panorama. We give two examples, and each example shows stitching results of 4 different frames using Perazzi et al.'s [17] method and our rectangling respectively.

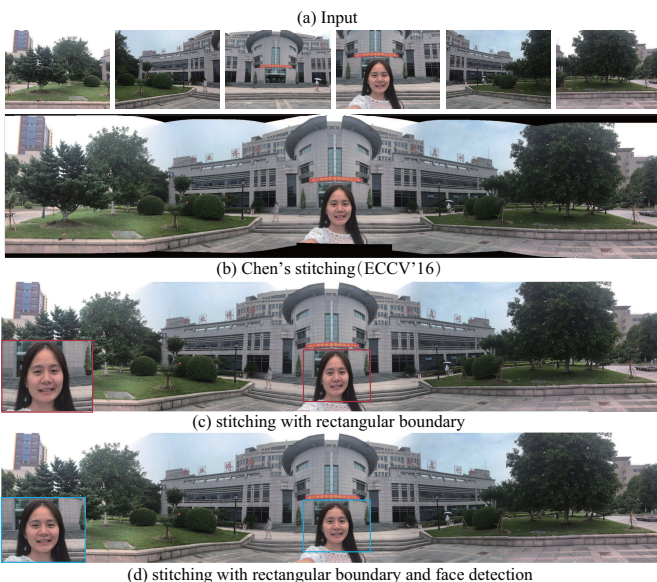


Fig. 9. Application of Selfie panorama. (a) Initial stitching results with irregular boundaries. (b) Results of our stitching with regular boundary, which distorts the human face. (c) Results of our stitching with regular boundary and face detection, which can avoid the unwanted face distortion.

stitching cost 0.76s, which includes feature matching, line detection, energy construction and optimization. Then, the stitching with rectangular boundary constraint cost 0.49s, which include the irregular boundary extraction, boundary constraint construction and iterative optimization. Finally, with the warped vertices, texture mapping and blending are performed, and the time cost is 2.15s. In our two-step optimization, the energy terms are similar, thus we construct them only once. In addition, the energy terms are quadratic, thus can be efficiently solved. For our iterative optimization in the piecewise rectangling, results in each iteration are similar, thus we apply conjugate gradient method, which takes result of last iteration as input, thus can solve the optimization more efficiently.

#### 4.4 Limitations

Due to the free movement of hand-held cameras, panorama images has irregular boundaries and missing contents. Our piecewise rectangling stitching can effectively rectify these problems by warping-based optimizations with regular boundary constraints. However, there are still some limitations: (1) Similar to most warping-based methods, our method cannot well preserve all lines when there are many lines in local regions. (2) Our method may fail when there is strong structure near the intersection of neighboring meshes. See Fig. 11, the zoom-in view show that, our piecewise



Fig. 11. Failure case: when there is strong structure in the intersection of meshes, our method may fail to preserve the structure.

rectangling scheme may introduce unwanted distortion in order to preserve the rectangular boundaries.

## 5 CONCLUSION

In this paper, we have proposed an efficient approach for content-preserving stitching with the regular boundary constraint, thus can generate panorama images with regular boundaries. Our main contribution is to propose a global optimization which incorporates the regular boundary constraint in the framework of image stitching. Based on the traditional stitching with irregular boundaries, we analyze the warped meshes and extract the outer boundary by the polygon boolean operation. With the outer boundary, we setup the piecewise rectangular boundary constraint for the content-preserving stitching. Compare with He et al.'s panorama rectangling, our method is more robust and effective. Especially for panoramic scenes with missing content, our piecewise rectangling can not only regularize the stitching boundary as-much-as-possible, but avoids unwanted distortions. Experimental results and comparisons show that our method is effective and better than state-of-the-art methods. Some challenging examples show the robustness and practicability. We further apply our method to selfie panorama and video stitching, which demonstrates the versatility of our approach.

In the future, we will consider more features to improve the performance of panorama boundary rectangling, such as structure, saliency, scene analysis etc. For video stabilization and stitching, the warping-based method may also introduce the irregular boundaries. Regularizing the boundary of warped videos can preserve more content in a cropping window and improve the viewing experiences. However, for videos shot by freely moving hand-held cameras, it is difficult to define the regular boundary constraint, and maintain the spatial-temporal coherence. We leave these problems as our future work.

## ACKNOWLEDGMENTS

The authors would like to thank...

## REFERENCES

- [1] S. Yen, H. Yeh, and H. Chang, "Progressive completion of a panoramic image," *Multimedia Tools Appl.*, vol. 76, no. 9, pp. 11 603–11 620, 2017.
- [2] C. Barnes, E. Shechtman, A. Finkelstein, and D. B. Goldman, "Patchmatch: a randomized correspondence algorithm for structural image editing," *ACM Trans. Graph.*, vol. 28, no. 3, pp. 24:1–24:11, 2009.
- [3] K. He, H. Chang, and J. Sun, "Rectangling panoramic images via warping," *ACM Trans. Graph.*, vol. 32, no. 4, pp. 79:1–79:10, 2013.
- [4] Y. Chen and Y. Chuang, "Natural image stitching with the global similarity prior," in *Computer Vision - ECCV 2016 - 14th European Conference, Amsterdam, The Netherlands, October 11-14, 2016, Proceedings, Part V*, 2016, pp. 186–201.
- [5] R. Szeliski, "Image alignment and stitching: A tutorial," *Foundations and Trends in Computer Graphics and Vision*, vol. 2, no. 1, 2006.
- [6] M. Brown and D. G. Lowe, "Automatic panoramic image stitching using invariant features," *International Journal of Computer Vision*, vol. 74, no. 1, pp. 59–73, 2007.
- [7] J. Gao, S. J. Kim, and M. S. Brown, "Constructing image panoramas using dual-homography warping," in *IEEE Conference on Computer Vision and Pattern Recognition (CVPR)*, 2011, pp. 49–56.
- [8] J. Zaragoza, T. Chin, Q. Tran, M. S. Brown, and D. Suter, "As-projective-as-possible image stitching with moving DLT," *IEEE Trans. Pattern Anal. Mach. Intell.*, vol. 36, no. 7, pp. 1285–1298, 2014.
- [9] C. C. Lin, S. U. Pankanti, K. N. Ramamurthy, and A. Y. Aravkin, "Adaptive as-natural-as-possible image stitching," in *IEEE Conference on Computer Vision and Pattern Recognition (CVPR)*, 2015, pp. 1155–1163.
- [10] S. Li, L. Yuan, J. Sun, and L. Quan, "Dual-feature warping-based motion model estimation," in *2015 IEEE International Conference on Computer Vision, ICCV 2015, Santiago, Chile, December 7-13, 2015*, 2015, pp. 4283–4291.
- [11] C. Chang, Y. Sato, and Y. Chuang, "Shape-preserving half-projective warps for image stitching," in *2014 IEEE Conference on Computer Vision and Pattern Recognition, CVPR 2014, Columbus, OH, USA, June 23-28, 2014*, 2014, pp. 3254–3261.
- [12] F. Zhang and F. Liu, "Parallax-tolerant image stitching," in *2014 IEEE Conference on Computer Vision and Pattern Recognition, CVPR 2014, Columbus, OH, USA, June 23-28, 2014*, 2014, pp. 3262–3269.
- [13] K. Lin, N. Jiang, L. Cheong, M. N. Do, and J. Lu, "SEAGULL: seam-guided local alignment for parallax-tolerant image stitching," in *Computer Vision - ECCV 2016 - 14th European Conference, Amsterdam, The Netherlands, October 11-14, 2016, Proceedings, Part III*, 2016, pp. 370–385.
- [14] J. Li, Z. Wang, S. Lai, Y. Zhai, and M. Zhang, "Parallax-tolerant image stitching based on robust elastic warping," *IEEE Trans. Multimedia*, vol. 20, no. 7, pp. 1672–1687, 2018.
- [15] B. He and S. Yu, "Parallax-robust surveillance video stitching," *Sensors*, vol. 16, no. 1, p. 7, 2016.
- [16] X. Yin, W. Li, B. Wang, Y. Liu, and M. Zhang, "A novel video stitching method for multi-camera surveillance systems," *TIIS*, vol. 8, no. 10, pp. 3538–3556, 2014.
- [17] F. Perazzi, A. Sorkine-Hornung, H. Zimmer, P. Kaufmann, O. Wang, S. Watson, and M. H. Gross, "Panoramic video from unstructured camera arrays," *Comput. Graph. Forum*, vol. 34, no. 2, pp. 57–68, 2015.
- [18] D. Anguelov, C. Dulong, D. Filip, C. Früh, S. Lafon, R. Lyon, A. S. Ogale, L. Vincent, and J. Weaver, "Google street view: Capturing the world at street level," *IEEE Computer*, vol. 43, no. 6, pp. 32–38, 2010.
- [19] Z. Zhu, J. Lu, M. Wang, S. Zhang, R. R. Martin, H. Liu, and S. Hu, "A comparative study of algorithms for realtime panoramic video blending," *IEEE Trans. Image Processing*, vol. 27, no. 6, pp. 2952–2965, 2018.
- [20] X. Meng, W. Wang, and B. Leong, "Skystitch: A cooperative multi-uav-based real-time video surveillance system with stitching," in *Proceedings of the 23rd Annual ACM Conference on Multimedia Conference, MM '15, Brisbane, Australia, October 26 - 30, 2015*, 2015, pp. 261–270.
- [21] M. A. El-Saban, M. Ezz, A. Kaheel, and M. Refaat, "Improved optimal seam selection blending for fast video stitching of videos captured from freely moving devices," in *18th IEEE International Conference on Image Processing, ICIP 2011, Brussels, Belgium, September 11-14, 2011*, 2011, pp. 1481–1484.
- [22] K. Lin, S. Liu, L. Cheong, and B. Zeng, "Seamless video stitching from hand-held camera inputs," *Comput. Graph. Forum*, vol. 35, no. 2, pp. 479–487, 2016.
- [23] H. Guo, S. Liu, T. He, S. Zhu, B. Zeng, and M. Gabbouj, "Joint video stitching and stabilization from moving cameras," *IEEE Trans. Image Processing*, vol. 25, no. 11, pp. 5491–5503, 2016.
- [24] Y. Nie, T. Su, Z. Zhang, H. Sun, and G. Li, "Dynamic video stitching via shakiness removing," *IEEE Trans. Image Processing*, vol. 27, no. 1, pp. 164–178, 2018.
- [25] R. G. von Gioi, J. Jakubowicz, J. Morel, and G. Randall, "LSD: A fast line segment detector with a false detection control," *IEEE Trans. Pattern Anal. Mach. Intell.*, vol. 32, no. 4, pp. 722–732, 2010.

- [26] S. Liu, L. Yuan, P. Tan, and J. Sun, "Bundled camera paths for video stabilization," *ACM Trans. Graph.*, vol. 32, no. 4, pp. 78:1–78:10, 2013.
- [27] T. Igarashi, T. Moscovich, and J. F. Hughes, "As-rigid-as-possible shape manipulation," *ACM Trans. Graph.*, vol. 24, no. 3, pp. 1134–1141, 2005.
- [28] T. Igarashi and Y. Igarashi, "Implementing as-rigid-as-possible shape manipulation and surface flattening," *J. Graphics, GPU, & Game Tools*, vol. 14, no. 1, pp. 17–30, 2009.
- [29] F. Martínez, A. J. Rueda, and F. R. Feito, "A new algorithm for computing boolean operations on polygons," *Computers & Geosciences*, vol. 35, no. 6, pp. 1177–1185, 2009.
- [30] J. Huang, S. B. Kang, N. Ahuja, and J. Kopf, "Image completion using planar structure guidance," *ACM Trans. Graph.*, vol. 33, no. 4, pp. 129:1–129:10, 2014.